

# Unitarity effects in hard diffraction at HERA

A.B. KAIDALOV<sup>a,b</sup>, V.A. KHOZE<sup>a,c</sup>, A.D. MARTIN<sup>a</sup> AND M.G. RYSKIN<sup>a,c</sup>

<sup>a</sup> Department of Physics and Institute for Particle Physics Phenomenology,  
University of Durham, DH1 3LE, UK

<sup>b</sup> Institute of Theoretical and Experimental Physics, Moscow, 117259, Russia

<sup>c</sup> Petersburg Nuclear Physics Institute, Gatchina, St. Petersburg, 188300, Russia

## Abstract

We study how factorization breaking changes when going from diffractive deep inelastic scattering to diffractive photoproduction of dijets. These processes offer a sensitive probe of the interplay of soft and hard mechanisms in QCD. We demonstrate that unitarity effects are already important in the gluon distribution for  $x \lesssim 10^{-4}$ , for quite a wide range of  $Q^2$ .

## 1 Introduction

The investigation of hard diffractive processes initiated by real and virtual photons gives important information on the interplay of soft and hard dynamics in QCD. These processes have been actively studied at HERA [1]. The hard scale is defined either by the virtuality  $Q^2$  of a photon or by the  $p_T(E_T)$  of jets (in diffractive production of jets) or by the mass  $M_Q$  of a heavy quark (for heavy-flavour diffractive production). For large  $Q^2$  it is possible to prove a QCD-factorization theorem [2], which allows one to describe the inclusive diffractive dissociation of a photon in terms of quarks and gluons, and to predict the  $Q^2$ -evolution of their distributions. Description of these processes is usually carried out in terms of the partonic distributions in the Pomeron, and corresponds to the diagram of Fig. 1. In the simplest approximation the exchange of a single, factorizable Pomeron Regge-pole  $P$  is assumed. We discuss the validity of this approximation at the end of the article. On the other hand, the QCD factorization theorem is not valid for diffractive dissociation at small  $Q^2$ , or for hard diffraction in hadronic interactions; see, for example, Refs. [2]–[5]. Rather, multi-Pomeron exchanges (of the type

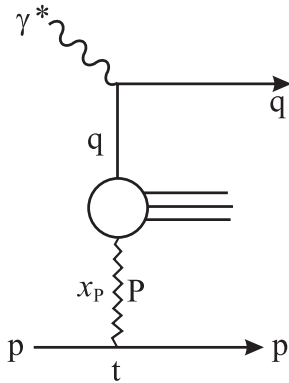


Figure 1: The simplest diagram for inclusive diffractive jet production in DIS at HERA.  $x_P$  is the fraction of the longitudinal momentum of the proton carried by the Pomeron  $P$ .

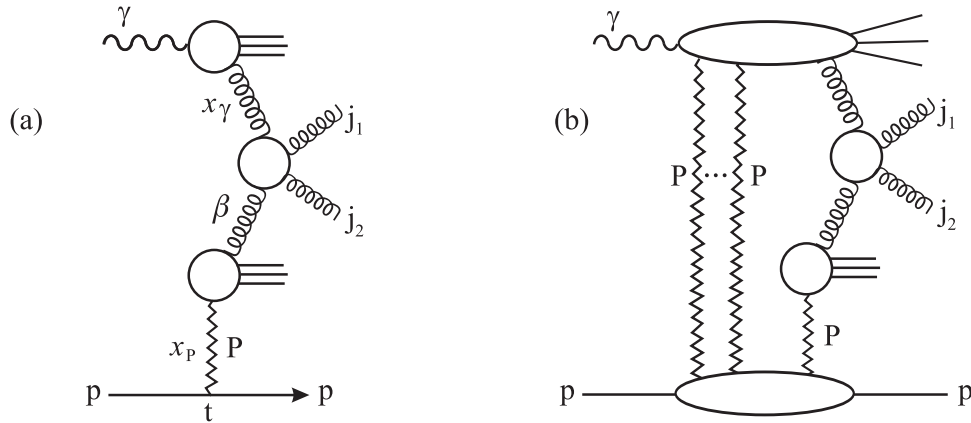


Figure 2: Diffractive dijet production at HERA from a *resolved* photon.  $x_\gamma$  is the fraction of the photon's longitudinal momentum carried by the resolved gluon. Diagrams (a) and (b) show the single-Pomeron-exchange and the multi-Pomeron-exchange contributions, respectively. Similar diagrams apply to diffractive dijet production in  $pp$  collisions.

shown in Fig. 2(b) for dijet production) play an important role [2, 3, 4]. It was demonstrated by the CDF Collaboration [6] that partonic distributions in the Pomeron (extracted from analyses of diffractive production in DIS corresponding to the diagram of Fig. 1) lead, according to a naïve factorization prescription (Fig. 2(a)), to a cross section which is about a factor of ten larger than the experimental one. However, when multi-Pomeron  $t$ -channel exchange diagrams (Fig. 2(b)) are included using the framework of the Reggeon diagram technique [7], which takes into account  $s$ -channel unitarity, the discrepancy disappears and a good description of the CDF data is obtained [4]. It is informative to extend the analysis to other diffractive processes. We showed recently [8] that the apparent breaking of QCD factorization in double-Pomeron dijet production is also consistent with the same multi-Pomeron exchange model.

Here we address the question of whether such hard QCD factorization breaking takes place in photoproduction at very small values of Bjorken  $x$  at HERA. Experimental data for the diffractive photoproduction of dijets have been obtained recently at HERA [9, 10, 11]. We first comment on the interpretation of the recent H1 data [10, 11], and emphasize that the existing treatment does not lead to unique conclusions. We will consider a simple analysis of experimental data, which also includes information on dijet inclusive photoproduction. Theoretical predictions for cross section ratios will be given.

The second part of the paper is devoted to the important problem of unitarity effects (or multi-Pomeron exchanges) in the lower part of the diagram of Fig. 1. It will be demonstrated that they are already crucial for the distributions of gluons in the domain  $x \lesssim 10^{-4}$ , almost independent of  $Q^2$ . The relation of these effects to the ‘saturation’ of partonic distributions is discussed.

## 2 Diffractive DIS- and photo-production of dijets

Here we consider the diffractive production of dijets by real and virtual photons in more detail. Besides the diagram of Fig. 2(a), there is a large contribution to these processes from the diagram of Fig. 3, which describes dijet production by photon–gluon fusion. This is usually called the ‘direct’ contribution, while Fig. 2(a) is known as the ‘resolved’ contribution. For large  $Q^2$  the effect of the rescattering diagrams of Fig. 2(b) is expected to be small, and the cross section of diffractive dijet production can be written as a sum of two terms

$$d\sigma_D^{jj} = d\sigma_D^{jj(\text{dir})} + d\sigma_D^{jj(\text{res})} \quad (1)$$

with

$$d\sigma_D^{jj(\text{dir})} = \int dt \int_{x_P^{\min}}^{x_P^{\max}} dx_P F_P(x_P, t) \beta f_P^g(\beta, \mu^2) \sigma_{\gamma g}^{j_1 j_2}(E_{1T}, E_{2T}, M_{12}^2, \dots) d^n \tau \quad (2)$$

$$d\sigma_D^{jj(\text{res})} = \int dt \int_{x_P^{\min}}^{x_P^{\max}} dx_P F_P(x_P, t) \beta f_P^g(\beta, \mu^2) x_\gamma f_{\gamma^*}^i(x_\gamma, \mu^2) \sigma_{ig}^{j_1 j_2}(E_{1T}, E_{2T}, M_{12}^2, \dots) d^n \tau \quad (3)$$

where  $x_P = (Q^2 + M_X^2)/(Q^2 + W^2)$  is the fraction of the longitudinal momentum of the proton carried by the Pomeron, and  $\beta = (Q^2 + M_{12}^2)/(Q^2 + M_X^2)$  is the fraction of the Pomeron

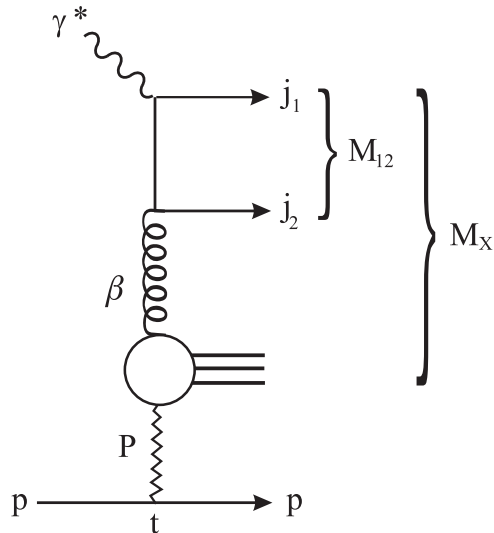


Figure 3: Diffractive dijet production at HERA via a *direct* photon interaction.

momentum carried by the gluon. Here,  $W$  is the total c.m. energy of the  $\gamma p$  system,  $M_X$  is the mass of the diffractively-produced system and  $M_{12}$  is the dijet mass. Also,  $x_g = x_P \beta = (Q^2 + M_{12}^2)/(Q^2 + W^2)$  is the fraction of the proton momentum carried by the gluon. Finally,  $\tau$  denotes all the variables that characterize the observed dijet system.

In (3),  $f_{\gamma^*}^i(x_\gamma, \mu^2)$  is the distribution of parton  $i$  in the virtual photon carrying a fraction  $x_\gamma$  of its momentum. The Pomeron flux factor,  $F_P(x_P, t)$ , and distribution of gluons in the Pomeron,  $f_P^g(\beta, \mu^2)$ , were determined from the analysis of data for the inclusive diffractive dissociation of a virtual photon [12, 13]. We take the scale  $\mu^2 = Q^2 + \frac{1}{4}(E_{1T} + E_{2T})^2$ . Until recently there was a rather large uncertainty in the determination of the gluonic content of the Pomeron. This uncertainty has been reduced in a recent LO and NLO analysis by the H1 Collaboration [13], which we will use in the following.

The experimental situation concerning evidence for factorization breaking in the diffractive photoproduction of dijets is far from clear. The current status can be summarized as follows. It was shown in Ref. [10] that the distribution of gluons from the new H1 analysis [13] gives a prediction for the cross section of dijet production in DIS, which is about 30% below the experimental results. However, this prediction was obtained in a LO QCD calculation, and NLO corrections can lead to an increase in the cross section, as was demonstrated for inclusive dijet production [14]. These effects are especially important in the small  $x_\gamma$  region where the resolved contribution mimics higher-order effects. On the other hand, the new analysis predicts the cross section for the photoproduction of dijets to be about 30% above experimental data. In this case, higher order corrections can also be large and, moreover, the resolved contribution of Fig. 2(a), which is not well determined at present, is rather substantial (especially at small  $x_\gamma$ ). Thus, in our opinion, in this situation it is difficult to draw a definite conclusion on the role of

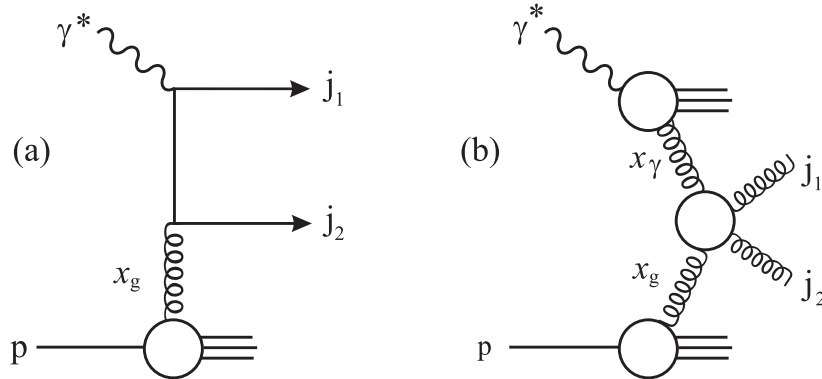


Figure 4: Schematic diagrams for inclusive dijet production at HERA. This process is compared in the text to diffractive dijet production. Diagrams (a) and (b) show the direct and resolved photon contributions respectively.

multi-Pomeron effects in  $\gamma P$ -dijet production. In particular, the conclusion of Refs. [11, 15] that there is an extra suppression of the  $\gamma P$  interaction by a factor  $1.8 \pm 0.45$ , which is independent of  $x_\gamma$ , should be treated with caution.

In order to clarify the situation we use a method, similar to that proposed by the CDF group for  $p\bar{p}$  collisions [6], which includes extra information on totally inclusive dijet production. The last process is described by the diagrams shown in Fig. 4. The upper parts of these diagrams have the same structure as the diagrams of Fig. 2(a) and Fig. 3 and differ only in the lower parts, which now depend on the distribution of gluons<sup>1</sup> in the proton, rather than those in the Pomeron. As a consequence, most quantities cancel in the ratio of diffractive and inclusive dijet production. Indeed, we obtain

$$R \equiv \frac{d\sigma_D^{jj}(\tau)}{d\sigma^{jj}(\tau)} = \frac{\tilde{F}_P^g(x_g, \mu^2)}{x_g f_P^g(x_g, \mu^2)}, \quad (4)$$

where the distribution of gluons in the diffractive process (containing a rapidity gap) is given by

$$\tilde{F}_P^g(x_g, \mu^2) = \int dt \int_{x_P^{\min}}^{x_P^{\max}} dx_P F_P(x_P, t) f_P^g(\beta, \mu^2), \quad (5)$$

with  $x_P^{\min} = x_g$  ( $\beta = 1$ ) and where  $x_P^{\max}$  is usually chosen to correspond to the experimental requirement on the rapidity gap. Note that, although  $R$  does not depend explicitly on the variable  $x_\gamma$ , this dependence appears due to kinematic correlations between the different variables. For example, since  $M_{12}^2$  is strongly peaked near the value related to the experimental lower cutoff, an  $x_\gamma$  dependence arises via  $x_\gamma x_g W^2 = M_{12}^2$ .

To predict the ratio  $R$  of the experimental cross sections, (4), we need to choose the input for  $F_P(x_P, t)$  and the distribution of gluons in the Pomeron. Here we used a factorized expression

<sup>1</sup>For very small  $x_g$ , which is relevant to the present analysis, gluons give the dominant contribution.

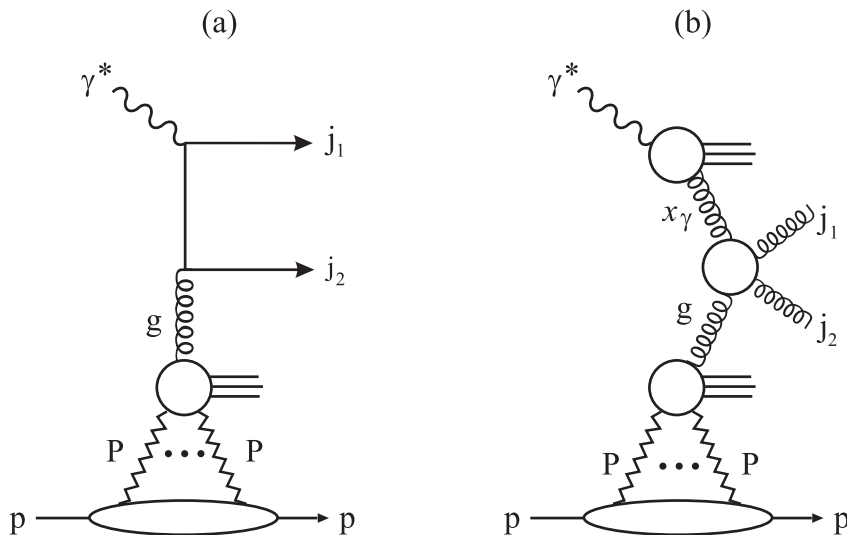


Figure 5: Multi-Pomeron contributions to inclusive dijet production.

in terms of the variables  $x_P$  and  $\beta$ , which corresponds to the exchange of a single Pomeron pole  $P$ , and which was used in analysis of experimental data<sup>2</sup>. In general, we can have more complicated, unfactorizable forms (see Fig. 5) but the same analysis of the ratio  $R$  still holds.

The theoretical prediction for the ratio  $R$  is shown by the continuous curve in Fig. 6. It is calculated using  $F_P$  and  $f_P^g$  given in Ref. [13] and  $f_p^g$  from Ref. [16], together with the experimental cuts of the H1 dijet experiment [11]. As the result is sensitive to experimental cuts it would be desirable to repeat the calculation of  $R$  using a Monte Carlo with the exact data cuts.

So far we have considered the large  $Q^2$  region, where the contributions of the diagrams of Fig. 2(b), with unitarity corrections, are expected to be small. For small values of  $Q^2$  (or real photons) these corrections should be taken into account. However these corrections influence mainly the production of dijets by *resolved* photons, which takes place mostly at small and moderate values of  $x_\gamma$ . For *direct* production, via Fig. 3, the rescattering corrections are small. It is worthwhile to recall the reason. First, the cross section of dijet rescattering is proportional to  $1/E_T^2$  and therefore the contribution of Fig. 2(b) is negligible. Next, it is important to note that the parton distributions of the Pomeron were measured in *direct* inclusive processes such as those shown in Figs. 3 and 5(a). Thus they effectively include the multi-Pomeron effects shown in Fig. 5, as well as the multi-Pomeron counterpart to Fig. 2(b) for the ‘direct’ process. The direct process is thus not suppressed by any additional rescattering corrections, as all such effects are already embodied in the normalisation of the effective Pomeron structure functions.

These corrections, which are sometimes called ‘the survival probability of rapidity gaps’

<sup>2</sup>For not too small values of  $x_P \sim 0.1$ , the contributions of secondary Reggeons can be important, and are usually included in the data analysis [12, 13].

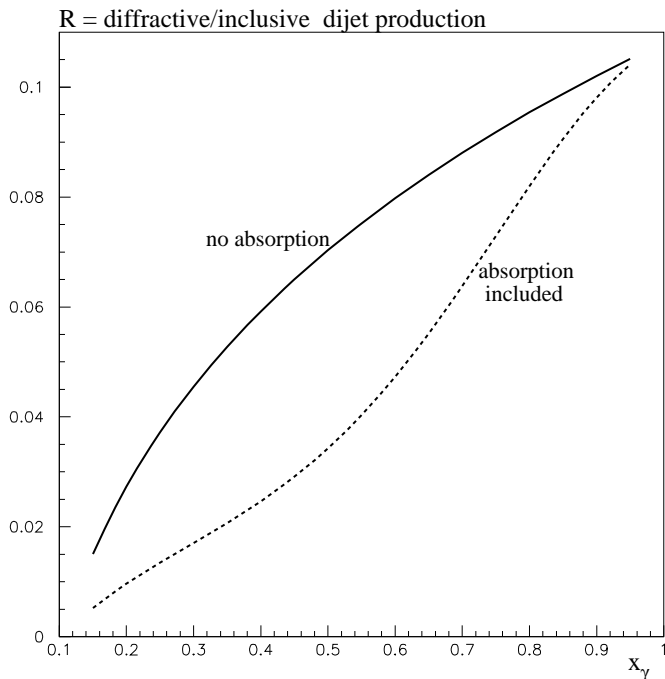


Figure 6: The predictions for the ratio,  $R$ , of diffractive and inclusive dijet photoproduction at HERA, of (4), as a function of  $x_\gamma$ . The curves have been calculated using the Pomeron flux and gluon distribution in the Pomeron of Refs. [13], and correspond to a  $\gamma$ -proton c.m. energy  $W = 205$  GeV, dijet mass  $M_{12} = 12$  GeV,  $x_P^{\max} = 0.03$  and scale  $\mu^2 = 15$  GeV<sup>2</sup>. For the gluon distribution in the proton we conservatively use that of CTEQ6M partons [16]. The use of the MRST2001 or MRST2002 [17] gluons gives a value of  $R$  which is a bit larger. The predictions based on single-Pomeron and multi-Pomeron exchange are shown as continuous and dashed curves respectively. The ratio  $R$  of the high  $Q^2$  processes is not expected to have absorptive corrections, and hence should follow the continuous curve.

or ‘the screening corrections from the underlying events’, suppress the cross section for hard diffractive processes. A two-channel eikonal model [18], with parameters tuned to fit all soft  $pp$  (and  $p\bar{p}$ ) data, has been used to predict the suppression factors for various hard diffractive processes. This model was used for the description of the diffractive production of jets in  $p\bar{p}$  interactions [4]. Here we apply the model to the photoproduction of dijets<sup>3</sup>. To describe the photon–proton interaction we use the generalized vector dominance model. We tune the  $\rho$ -meson Pomeron vertex so that, at  $W = 200$  GeV,  $\sigma^{\text{tot}}(\rho p) = 34$  mb and the slope of the cross section for diffractive  $\rho$  photoproduction is  $B = 11.3$  GeV<sup>-2</sup>, to be consistent with the HERA data [20]. The parameter  $\gamma$  in the two-channel eikonal (eq. (33) of Ref. [18]) was taken to be  $\gamma = 0.6$  to account for the large probability of  $\rho$  meson excitation in comparison with that for the proton.

In the *ideal* theoretical limit, using the above model we find that the difference between the predictions for  $R$  for DIS and for photoproduction is a common suppression factor of 0.34 for photoproduction for all  $x_\gamma$ , except for the ‘direct’ photon contribution at  $x_\gamma = 1$  which has no suppression. However, in *reality*, the ‘direct’ contribution is smeared by the experimental resolution and uncertainties connected with the jet finding algorithms. In an attempt to account for the smearing, we assume that the direct contribution is of the Gaussian form  $\exp(-6(1 - x_\gamma)^2)$ , chosen to agree with the observations of Fig. 4 of Ref. [11].

With this smearing factor, and using the same experimental cuts for photoproduction as for the large  $Q^2$  DIS data, we predict the suppression corresponding to the dashed curve in Fig. 6. For small  $x_\gamma \lesssim 0.3$ , away from the smearing effects, we see the 0.34 suppression factor. That is the dashed “photoproduction” curve lies a factor 3 below the “high  $Q^2$ ” continuous curve, which does not suffer unitarity corrections.

We believe that this method of analysis is simple, informative and convenient from both the theoretical and experimental points of view, as most of the theoretical uncertainties (as well as some experimental systematics) cancel in the ratio  $R$ . Moreover, it can be used in other situations, such as, for example, the diffractive production of charm [21, 22].

### 3 Unitarization of the gluon distribution at small $x$

Now we consider some problems with existing parameterizations of the quantity  $\tilde{F}_P^g(x, \mu^2)$  of (5). By definition the quantity  $R$  is less than unity. However, for  $\alpha_P(0) = 1.173$  in the Pomeron flux factor and with the existing expressions for  $f_P^g(\beta, \mu^2)$  [13], the function  $R$  quickly increases as  $x \rightarrow 0$ . This can be seen from Fig. 7, which shows the ratio  $R$  for different values of  $\mu^2$ . Indeed we see that  $R$  approaches, or even exceeds, unity in the region<sup>4</sup> of  $10^{-4} \lesssim x_g \lesssim 10^{-5}$

<sup>3</sup>This model was applied to the photoproduction of jets separated by a large rapidity gap in Ref. [19].

<sup>4</sup>Of course, in this region the curves are particularly sensitive to the choice of input for the Pomeron flux, the Pomeron and proton gluon densities, and the value of  $x_P^{\text{max}}$ , but all reasonable choices indicate a violation of unitarity similar to that shown in Fig. 7.



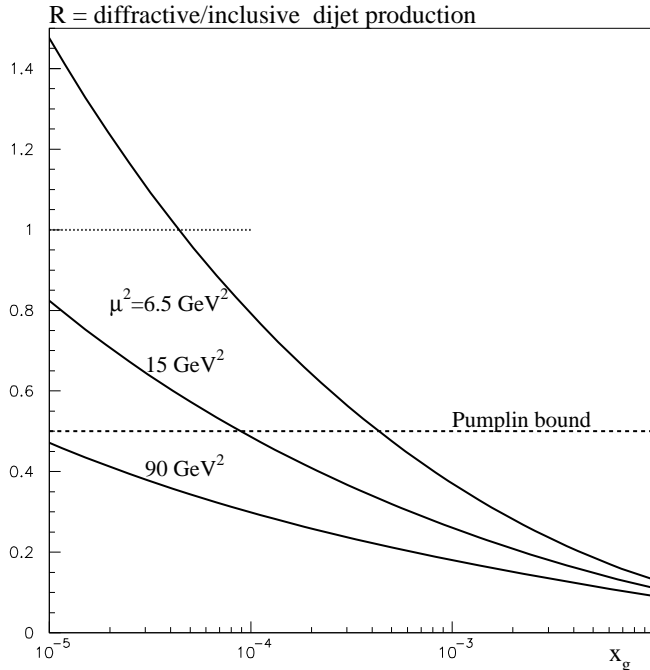


Figure 7: Predictions for the ratio  $R$  of diffractive and inclusive dijet production, of (4), shown as a function of  $x_g$  for different scales  $\mu^2$ , with  $x_P^{\max} = 0.1$ . Absorptive corrections are neglected.

for quite a range of virtualities  $\mu^2$ . This means that the application of the single Regge pole approximation in the small  $x$  region is not valid and leads to a violation of unitarity. The diagrams of Fig. 5, which take into account multi-Pomeron exchanges, must be included (as, for example, has been done in Ref. [23]) in order to ensure that  $R < 1$ , and to restore unitarity<sup>5</sup>.

Comparing the diagrams of Figs. 5 and 4, we may say that the value of  $R$  of (4) represents the ratio of the cross section for gluon diffractive dissociation (the lower part of Fig. 5) to the total gluon–proton cross section. In analogy with hadronic interactions, it is reasonable to believe that diffractive processes are less than one half of the total gluon–proton cross section [25], and thus that  $R \leq \frac{1}{2}$ . From Fig. 7 we see that, for gluons, this bound is already exceeded for  $x_g \sim 10^{-4}$ . Moreover, the violation of unitarity appears in this region of  $x_g$  over a large interval of  $\mu^2$ . This is related to the fact that the diffractive production of states with small  $\beta$  is not a high-twist effect. Note that here we discuss the absorptive effect caused by the rescattering of intermediate partons (described by the multi-Pomeron exchange contributions shown in Fig. 5), and not the rescattering of the fast constituents of the photon. The rescattering of intermediate partons takes place at scales much smaller than the hard scale  $\mu^2$ . The main origin of the large

<sup>5</sup>See also the discussion of this problem in Ref. [24].

values of  $R$  (which indicate the violation of unitarity) is the power-like growth ( $x^{1-\alpha_P(0)}$ ) of the single-Pomeron-exchange amplitude. This growth must be tamed. As can be seen from Fig. 7, this effect is much more important in inelastic diffraction than in the total cross section or pure inclusive processes. In inclusive processes the absorptive corrections are small due to AGK cancellations [26]<sup>6</sup>. In the total cross section, or in inclusive DIS discussed here, part of the absorptive effect is mimicked by the input gluon distribution.

These observations may be important for understanding the problem of ‘saturation’ in heavy-ion collisions, and also in diffractive charm production at very small  $x$ .

## 4 Conclusions

The recent observation of diffractive dijet photoproduction, combined with the measurements of diffractive dijet DIS production, offers a unique opportunity to probe the special features of diffractive dynamics. We have emphasized that a good way to study the effects of factorization breaking due to rescattering (or, in other words, the suppression caused by absorptive corrections) is to take the ratio of the diffractive process to the corresponding inclusive production process, that is

$$R = \frac{\sigma(\text{diffractive})}{\sigma(\text{inclusive})} \quad (6)$$

of (4). A comparison of the predictions for  $R$  with the data, for both photoproduction and DIS, should be very informative. Moreover many theoretical uncertainties, and some experimental uncertainties, cancel in the ratio.

The high  $Q^2$  diffractive process, unlike diffractive photoproduction, is not expected to suffer rescattering corrections. Indeed in the ideal theoretical limit we predict

$$R(\text{photoprod.}) \simeq 0.34 R(\text{high } Q^2), \quad (7)$$

except at  $x_\gamma = 1$ , where the ratios are expected to be equal since there should be very small rescattering corrections to the ‘direct’ photon contribution. In practice the experimental resolution and jet finding algorithms have the effect of smearing the ‘direct’ contribution. We estimated this effect and showed the resulting predictions for  $R$  in Fig. 6. The 0.34 suppression of diffractive photoproduction due to absorptive corrections is clearly evident for small  $x_\gamma \lesssim 0.3$ , where smearing effects are negligible. Since the predictions for  $R$  depend on the experimental cuts (in particular on the value of  $x_P^{\text{max}}$ ) the curves should be recalculated to match the conditions of the experiment, including the smearing of the  $x_\gamma$  distribution. However the ratio of ratios,  $R(\text{photoprod.})/R(\text{high } Q^2)$ , for  $x_\gamma \lesssim 0.3$  should be a reasonably stable prediction.

Clearly it will be interesting to measure  $R$  as a function of  $Q^2$ . At large  $Q^2$  the absorptive corrections are expected to be negligible and the prediction is given by the factorization theorem,

---

<sup>6</sup>Indeed soft rescattering does not alter the distribution of high  $E_T$  jets in inclusive processes, but fills in and destroys the rapidity gap in diffractive reactions.

that is the continuous curve in Fig. 6. However as  $Q^2$  decreases we would expect the prediction for  $R$  to tend gradually towards the dashed photoproduction curve. Recall that for  $x_\gamma \gtrsim 0.5$  the values of  $R$  have an additional uncertainty due to the contamination of the ‘direct’ photon contribution.

The above behaviour of  $R$  is also expected for diffractive charm production. However, in this case, the relative contribution of the ‘direct’ photon process (where the absorptive effect is expected to be small) is enhanced by a colour factor.

The value of  $R$  is proportional to the effective number of gluons coming from the Pomeron, and may be considered as the ratio of gluon diffractive dissociation to the total gluon–proton cross section. At relatively low scales, we see from Fig. 7, the ratio in the absence of absorptive corrections exceeds the Pumplin bound,  $R < \frac{1}{2}$ , already at  $x_g \sim 10^{-4}$ . Thus it reveals the need for absorptive corrections<sup>7</sup> in diffractive processes already at HERA energies.

## Acknowledgements

We thank Sebastian Schätzel for information. ABK and MGR would like to thank the IPPP at the University of Durham for hospitality. This work was supported by the UK Particle Physics and Astronomy Research Council, by grants INTAS 00-00366, RFBR 00-15-96786, 01-02-17383 and 01-02-17095, and by the Federal Program of the Russian Ministry of Industry, Science and Technology 40.052.1.1.1112 and SS-1124.2003.2.

## References

- [1] ZEUS Collaboration: M. Derrick et al., *Zeit. Phys.* **C68** (1995) 569; *Eur. Phys. J.* **C6** (1999) 43;  
H1 Collaboration: T. Ahmed et al., *Phys. Lett.* **B348** (1995) 681.
- [2] J.C. Collins, *Phys. Rev.* **D57** (1998) 3051 (Erratum: *ibid.* **D61** (2000) 019902).
- [3] E. Gotsman, E. Levin and U. Maor, *Phys. Lett.* **B452** (1999) 387; *Phys. Rev.* **D60** (1999) 094011 and references therein.
- [4] A.B. Kaidalov, V.A. Khoze, A.D. Martin and M.G. Ryskin, *Eur. Phys. J.* **C21** (2001) 521.
- [5] A. Bialas, *Acta Phys. Polon.* **B33** (2002) 2635.
- [6] CDF Collaboration: T. Affolder et al., *Phys. Rev. Lett.* **84** (2000) 5043.

---

<sup>7</sup>The multi-Pomeron contributions in Fig. 5.

- [7] V.N. Gribov, Sov. Phys. JETP **19** (1969) 483.
- [8] A.B. Kaidalov, V.A. Khoze, A.D. Martin and M.G. Ryskin, Phys. Lett. **B559** (2003) 235.
- [9] ZEUS Collaboration: J. Breitweg et al., Eur. Phys. J. **C5** (1998) 41.
- [10] H1 Collaboration: C. Adloff et al., Eur. Phys. J. **C6** (1999) 421; Eur. Phys. J. **C20** (2001) 29.
- [11] H1 Collaboration, abstract 987 presented at ICHEP02, Amsterdam, July 2002.
- [12] H1 Collaboration: C. Adloff et al., Z. Phys. **C76** (1997) 613.
- [13] H1 Collaboration: C. Adloff et al., abstract 980 presented at ICHEP02, Amsterdam, July 2002.
- [14] H1 Collaboration: C. Adloff et al., Phys. Lett. **B542** (2002) 193.
- [15] H1 Collaboration: S. Schätzel, Talk at DIS2003.
- [16] CTEQ Collaboration: J. Pumplin et al., JHEP **0207** (2002) 012.
- [17] A.D. Martin, R.G. Roberts, W.J. Stirling and R.S. Thorne, Eur. Phys. J. **C23** (2002) 73; *ibid.*, **C28** (2003) 455.
- [18] V.A. Khoze, A.D. Martin and M.G. Ryskin, Eur. Phys. J. **C18** (2000) 167.
- [19] L. Motyka, A.D. Martin and M.G. Ryskin, Phys. Lett. **B502** (2002) 107.
- [20] ZEUS Collaboration: J. Breitweg et al., Eur. Phys. J. **C2** (1998) 247; H1 Collaboration, C. Adloff et al., Eur. Phys. J. **C13** (2000) 371.
- [21] H1 Collaboration: C. Adloff et al., Z. Phys. **C72** (1996) 593.
- [22] ZEUS Collaboration: J. Breitweg et al., Phys. Lett. **B407** (1997) 402; Eur. Phys. J. **C6** (1999) 67.
- [23] A. Capella, E.G. Ferreira, A.B. Kaidalov and C.A. Salgado, Phys. Rev. **D63** (2001) 054010.
- [24] L. Frankfurt, M. Strikman and M. Zhalov, [arXiv:hep-ph/0304301](https://arxiv.org/abs/hep-ph/0304301).
- [25] J. Pumplin, Phys. Rev. **D8** (1973) 2899.
- [26] V. Abramovsky, V.N. Gribov and O.V. Kancheli, Sov. J. Nucl. Phys. **18** (1974) 308.